Tellus (2005), 57A, 84–99
Printed in UK. All rights reserved

TELLUS

Thermohaline loops, Stommel box models, and the Sandström theorem

By CARL WUNSCH*, *Department of Earth, Atmospheric and Planetary Sciences, Massachusetts Institute of Technology, Cambridge, MA 02139, USA*

(Manuscript received 22 January 2004; in final form 19 August 2004)

ABSTRACT

The Stommel two-box, two flow-regime box model is kinematically and dynamically equivalent to the flow in a one-dimensional fluid loop, although one having awkward and extreme mixing coefficients. More generally, such a loop, when heated and cooled at the same geopotential, provides a simple example of the working of the Sandström theorem, with flow intensity capable of increasing or decreasing with growing diffusion. Stress dominates real oceanic flows, and its introduction into the purely thermally driven loop generates oscillations, multiple states, and instabilities at low diffusivity. When, within the Boussinesq approximation, salinity forcing and mixed boundary conditions are further introduced, an intricate pattern of response appears, dependent upon at least five non-dimensional parameters, including the time of onset of salinity forcing. The ability, in a one-dimensional loop, to produce such a rich array of dynamical behaviors, dependent in detail upon the problem parameters, suggests that in the absence of any general results relating one- to three-dimensional fluid flows, identification of the time-dependent behavior of a GCM with that of the one-dimensional loop Stommel models should be regarded as still primarily speculation.

1. Introduction

This paper began as an attempt to find a simple teaching demonstration of the operation of the so-called Sandström theorem for the behavior of a fluid heated and cooled at the same level, and an independent effort to understand the impact of finite stratification on the two-box model of Stommel (1961, hereafter S61), commonly employed as an analog of multistate ocean circulations. It fairly soon became clear that the two goals were the same, and they have thus been combined here into the study of flow in a one-dimensional loop.

A surprisingly large literature exists concerning one-dimensional fluid loops. The volume of papers ceases to be surprising when one begins to appreciate the complexity of such flows in the presence of heat and salt sources. Although the original motivation of this paper was as described, the final goals are: (1) to reduce the loop system, in the presence of heat and salt, to what may be its simplest possible configuration; (2) to obtain a solution demonstrating the Sandström theorem; (3) to make explicit the connection between the S61 box model and the one-dimensional fluid loop, with emphasis on the role of mixing; (4) to study the influence of a wind stress analog on the system; (5) to question the analogies drawn between the behavior of three-dimensional time-dependent GCMs and the fluid loop flows.

The last point is perhaps the most important; we find that one-dimensional fluid loops with buoyancy forcing at a fixed depth display a remarkable range of oscillations and instabilities. Analogies are often drawn with the behavior of ocean GCMs by claims that the fluid loop (in the guise of the S61 model) has captured the basic physics. However, theories of the ocean circulation (e.g. Pedlosky, 1996) tend to emphasize the role of three-dimensionality and, particularly, the powerful role the wind-driven currents play in controlling both the circulation and its interaction with the atmosphere. It is difficult to imagine any one-dimensional circulation able to mimic the time-dependent, or stability, properties of an ocean circulation dominated by western boundary currents on the one hand, and a complex three-dimensional return flow on the other – even in a laminar regime. To the extent that such analogies can truly be drawn, one has achieved an exceedingly powerful simplification of a complex fluid problem that needs to be widely understood and celebrated.

One goal here is to show the great sensitivity of one-dimensional buoyancy and stress-driven models to specification in empirical parameters, such as the diffusion coefficients and stress. These models are of interest in their own right. Whether three-dimensional GCMs, with their multiplicity of pathways,

*Corresponding author.
e-mail: cwunsch@mit.edu

are likely to have a similar behavior is a question that will be raised again at the end.

2. A simple model

2.1. The loop

The study of fluid loops of such narrow cross-section that they can be considered governed by one-dimensional flow dynamics dates back at least to Jeffreys (1925). More recent interest arose with the pioneering papers of Keller (1966), Welander (1967), and Malkus (1972), and a large succeeding literature, some of which is discussed below. Thermally excited loops have major engineering applications in manufacturing, in heat exchangers, and the like (called 'thermosyphons') and three-dimensional extensions exist (e.g. Jiang and Shoji, 2003).

Consider the circular loop shown in Fig. 1, and the defining polar coordinate system, taking ϕ as measuring the angular distance from the top, positive in the counterclockwise direction. The radius is a, and the loop is supposed sufficiently thin that we can ignore all flows except w, in the azimuthal direction, and which of necessity, in the Boussinesq approximation, is a constant with ϕ. (w is a Poiseuille flow in a tube of vanishing cross-section.) A heating source exists at angle ϕ_+ and there is an equal and opposite cooling source at ϕ_-. Neither the notation nor the coordinate system for this geometry is universal in the literature.

Let density be a linear function of temperature, T, and salinity, S,

$$\rho(\phi, t) = \rho_0 [1 - \Delta_T T(\phi, t) + \Delta_S S(\phi, t)] \tag{1}$$

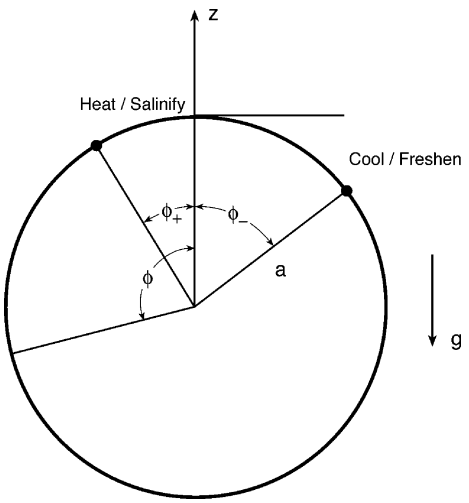

Fig 1. Coordinate system used to define the loop flow problem. ϕ is measured from the vertical, and heating and cooling sources appear at $\phi = \phi_\pm$. Radius is a, and the loop is sufficiently thin that there is no cross-loop dependence. ϕ_- is generally taken to be negative.

where Δ_T and Δ_S are the respective expansion/contraction coefficients, and ρ_0 is a constant. The governing thermal equation is

$$\frac{\partial T}{\partial t} + \frac{w}{a}\frac{\partial T}{\partial \phi} - \frac{\kappa_T}{a^2}\frac{\partial^2 T}{\partial \phi^2} = 2\pi H[\delta(\phi - \phi_+) - \delta(\phi - \phi_-)]h(t) + \gamma[T^*(\phi) - T(\phi)]. \tag{2}$$

$\delta(\phi)$ is the delta-function, and $h(t)$ is the Heaviside function, permitting the heat source and sink to turn on at $t = 0$, and to remain steady thereafter. H is a constant, γ is a coefficient with dimensions of reciprocal time, used to 'restore' $T(\phi)$ to a prescribed temperature field $T^*(\phi)$, and κ_T is the thermal diffusivity. Unlike most previous studies, delta-function sources are included here to permit easier separation of the behavior of the system with restoring terms from one with externally prescribed sources. The salinity field is governed by

$$\frac{\partial S}{\partial t} + \frac{w}{a}\frac{\partial S}{\partial \phi} - \frac{\kappa_S}{a^2}\frac{\partial^2 S}{\partial \phi^2} = 2\pi S_0[\delta(\phi - \phi_+) - \delta(\phi - \phi_-)]h(t - t_c), \tag{3}$$

where t_c permits the salinity sources to turn on at time $t_c \geq 0$. The salinity diffusivity, κ_S, could differ from that of temperature, permitting discussion of double-diffusive phenomena, but in this paper they are taken to be equal.

Dewar and Huang (1995) and Huang and Dewar (1996) have made the important point that the employment of salinity sources in eq. (3) corresponds to an oceanographically non-physical pseudo-salinity boundary condition (see also Huang, 1993). The ocean does not exchange salt with the atmosphere, only freshwater, i.e. mass. A mass source should appear in a different equation, that of continuity, which in the present case could be written

$$\frac{\partial (rw)}{r\partial r} + \frac{\partial w}{r\partial \phi} = 2\pi M_0[\delta(\phi - \phi_+) - \delta(\phi - \phi_-)] \times \delta(r - r_a)h(t - t_c), \tag{4}$$

where M_0 is a magnitude, and r_a is the outer radius of a torus centered at $r = a$, of finite diameter $2r_a$. The right-hand side of eq. (3) should then vanish. Dewar and Huang (1995) show that substitution of a pseudo-salinity boundary condition, for what they term the 'natural' boundary condition of mass flux, can lead to qualitatively different flows.

In the present situation, we will nonetheless use the pseudo-salinity boundary condition, primarily because it leads to the possibility of a nearly analytical solution procedure, in contrast to the use of eq. (4), and which appears to require a numerical solution almost at the outset. Furthermore, because almost all GCMs use pseudo-salinity boundary conditions and the Boussinesq approximation, and we seek to relate solutions here in part to their results, one can argue, with partial conviction, that retention of the common boundary condition renders the comparison more straightforward. Continuity then reduces simply to $\partial w/\partial \phi = 0$. The use of this condition does again raise the

general question, taken up at the end, of whether loop flows in any way do represent oceanic circulations.

The momentum equation in the Boussinesq approximation is

$$\frac{\partial w}{\partial t} = -\frac{\partial p}{a\rho_0 \partial \phi} + g[1 - \Delta_T T(\phi) + \Delta_S S(\phi)] \sin\phi - \varepsilon w + \tau \tag{5}$$

where p is the pressure, and ε is a Rayleigh friction coefficient acting on the along-loop flow. The second term on the right-hand side of eq. (5) is the azimuthal buoyancy force and τ is an externally prescribed stress assumed uniform along the flow path (unnecessary, but convenient).

Non-dimensionalization is useful, but there is not a unique best choice. Using primes for non-dimensional variables we put

$$T = \sqrt{\frac{\varepsilon a H}{g\Delta_T}} T', \qquad w = \sqrt{\frac{g\Delta_T a H}{\varepsilon}} w',$$

$$p = \rho_0 \sqrt{g\Delta_T \varepsilon a^3 H}\, p', \qquad t = \sqrt{\frac{\varepsilon a}{g\Delta_T H}} t',$$

$$\tau = \sqrt{ga\varepsilon\Delta_T H}\,\tau', \qquad S = S_0 \sqrt{\frac{\varepsilon a}{gH\Delta_T}} S'$$

which scale with the thermal source strength. A limitation of this scaling is its use of ε, which hides a Prandtl number dependence. Equations (2), (5) and (3) become

$$\frac{\partial T'}{\partial t'} + w' \frac{\partial T'}{\partial \phi} - R \frac{\partial^2 T'}{\partial \phi^2} = 2\pi[\delta(\phi - \phi_+) - \delta(\phi - \phi_-)]h(t) + \gamma'[T^{*'}(\phi) - T(\phi)], \tag{6}$$

$$\frac{\partial S'}{\partial t'} + w' \frac{\partial S'}{\partial \phi} - R_S \frac{\partial^2 S'}{\partial \phi^2} = 2\pi[\delta(\phi - \phi_+) - \delta(\phi - \phi_-)]h(t'), \tag{7}$$

$$F \frac{\partial w'}{\partial t'} = -\frac{\partial p'}{\partial \phi} + \sin\phi - T'(\phi)\sin\phi + DS'(\phi)\sin\phi - w' + \tau', \tag{8}$$

$$R = \sqrt{\frac{\varepsilon\kappa^2}{ga^3\Delta_T H}} = Ra^{-1}, \qquad R_S = \sqrt{\frac{\varepsilon\kappa_S^2}{ga^3\Delta_T H}},$$

$$P_r = a^2\varepsilon/\kappa, \qquad F = 1/(RP_r) = \sqrt{\frac{g\Delta_T H}{a\varepsilon^3}},$$

$$D = \frac{\Delta_S}{\Delta_T}\frac{S_0}{H}, \qquad \gamma' = \gamma\sqrt{\frac{\varepsilon a}{gH\Delta_T}}.$$

R and R_S are inverse Rayleigh numbers (Ra), and Pr is a Prandtl number. Note that the dimensional time-scale is a/w.

We define $p' = p'_0 + p'_1$, where

$$-\frac{\partial p'_0}{\partial \phi} + \sin\phi = 0.$$

This equation represents the rest hydrostatic pressure (noting that the sign of the pressure gradient reverses with the sign of ϕ.) This rest pressure can be ignored in what follows, and we will work only with p'_1, suppressing the subscript.

The algebra of this system is simplest if the heat and salt sources are both replaced by restoring conditions dependent only upon $\sin\phi$, or $\cos\phi$, as has been done in most previous studies; however, the physical motivation is then perhaps less transparent. Doing so also raises questions about the system energetics. Spatially limited sources permit unambiguous specification of the depth of heating/cooling, a major consideration in understanding the response. With restoring, the depths of heat entry/exit depend upon the flow itself, and thus we retain the explicit sources.

2.2. *Loop–Stommel model*

Before continuing, let us connect the loop to the S61 model. Since the introduction of the box model in S61, such constructs have been regarded as surrogates for the behavior of much more complicated dynamics of various climate states (e.g. Manabe and Stouffer, 1999). S61 explored the possibility of multiple states (of flow, temperature, and salinity) in a configuration governed only by the differing transfer rates of temperature and salt between the oceanic and external reservoirs. An important element of Stommel's original formulation (Fig. 2) is the existence of the two mixing propellers used to keep the boxes uniformly mixed as fluid flows between them. In S61, Stommel said little about these mixing devices, and they mainly disappeared in most subsequent discussions of, and elaborations on, the model, evidently being regarded as more or less incidental or uninteresting details of the problem. Many variations of the Stommel model have been proposed and used (reviewed by Whitehead, 1995 and Marotzke, 2000). Recent discussions of the oceanic meridional overturning circulation, however, for which the model is most widely regarded as a prototype (Munk and Wunsch, 1998; Huang, 1999; Nilsson and Walin, 2001; Wunsch and Ferrari, 2004) suggests that the mixing rates and distributions may, in practice, be the central element of the problem, essentially controlling both the nature and rates of flow.

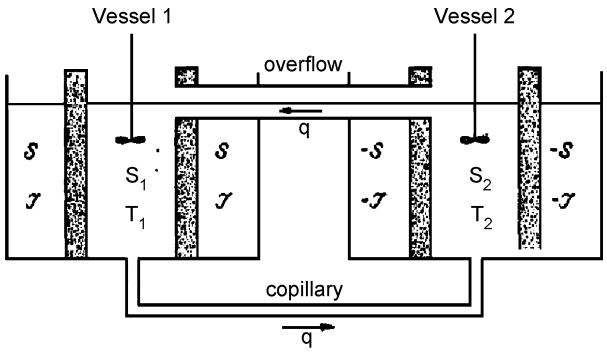

Fig 2. Model employed by S61 to analyze possible multistate flows. Note the mechanical mixing devices depicted as stirring the two reservoirs. Here the two reservoir values (S_i, T_i) are governed by the external reservoir values ($\mathcal{S}$, $\mathcal{T}$), the rate of lateral transfer (q), and the infinite mixing represented by the two propellors.

A number of authors have noticed the close relationship between the loop models and S61 (see, for example, Welander, 1985; Whitehead, 1995; Dewar and Huang, 1995). The S61 model is a form of rectangular loop, albeit with somewhat awkward conditions. In the present circular loop, we define

$$\begin{aligned} R_{61}(\phi) &= 0,\ \phi_- \le \phi \le \phi_+,\ 2\phi_+ \le \phi \le \pi,\ -\pi \le \phi \le \phi_-, \\ &= R_\infty,\ \phi_+ \le \phi \le 2\phi_+,\ 2\phi_- \le \phi \le \phi_-, \\ &\quad |\phi_\pm| \le \pi/2|,\ R_\infty \to \infty, \end{aligned} \tag{9}$$

that is, the diffusion (inverse Rayleigh number) vanishes in the upper part of the loop between the heat/salt sources, and in the corresponding, symmetrically placed, region at the bottom of the loop $2\phi_+ \le \phi \le \pi$, $-\pi \le \phi \le 2\phi_-$. Diffusion becomes arbitrarily large below the two source positions, in what corresponds to the S61 reservoirs. Omitting the sources, we can then write the heat diffusion equation as

$$\frac{\partial T'}{\partial t'} + w' \frac{\partial T'}{\partial \phi} - \frac{\partial}{\partial \phi}\left[R_{61}(\phi)\frac{\partial T'}{\partial \phi}\right] = \gamma'\left[T^{*'}(\phi) - T'(\phi)\right]. \tag{10}$$

$T^*(\phi)$ would be the constant T_1, $\phi_+ \le \phi \le 2\phi_+$, and $-T_1$, $2\phi_- \le \phi \le \phi_-$, to provide Stommel's forcing to external bath temperatures. A similar equation with restoring is written for salt (but see the comments by Dewar and Huang, 1995, concerning salinity conservation in that case). The momentum equation remains unchanged.

The focus of most discussion has been on the nature of the multiple states and transitions possible when both temperature and salinity boundary conditions are imposed, examining among other problems the use of so-called mixed boundary conditions when fluxes are used for salt or equivalent salt boundary conditions, and restoring is used for temperature (see Tziperman et al., 1994; Dewar and Huang, 1995; Huang and Dewar, 1996). A major limitation of most discussions of S61-like models is their omission of any role for the wind stress, although Stommel and Rooth (1968) showed that it had a profound effect on the flow properties. Given the dominant importance of the western boundary currents and their return flows in the oceanic general circulation, one of the more surprising features of many discussions of the ocean in climate change is the entire omission of the wind-driven circulation. Apart from these kinematic effects, the energetics of models lacking mechanical sources of energy (Paparella and Young, 2002; Wunsch and Ferrari, 2004), such as the wind and tides, are unrealistic. Models that simply omit the wind stress without any justification are not easy to interpret. Here we will try to partially remedy that lack. [A recent, entirely independent, attempt at adding wind effects by addition of a third box, is the paper of Pasquero and Tziperman (2004); Maas (1994) takes a very different approach.]

Some of the consequences of the results here concern the impact of temporally changing diffusion rates in an existing flow. Such a situation would be uncommon when the coefficients are molecular in origin. However, in oceanic and other models, these coefficients originate from 'eddy-mixing'. They are imposed through outside mechanical forces such as winds and tides (Munk and Wunsch, 1998; Huang, 1999; Paparella and Young, 2002; Wunsch and Ferrari, 2004), and the extent to which a flow can undergo major transitions through apparently small effects becomes of concern. (An example is the possibility of abrupt change in deep ocean mixing from tides when continental shelves are added or removed by sea level changes. This problem will be discussed elsewhere.) To the degree that oceanic mixing is a consequence of the wind stress (see Wunsch (2005)), it is yet another reason for regarding its presence in models as essential.

Given that the S61 model is dynamically and kinematically equivalent to a loop, we can analyze the flow behavior in a more transparent way than is possible in the original S61 context with discontinuous, infinitely large, or zero, inverse Rayleigh numbers within the loop.

3. Thermal driving alone: no relaxation

3.1. Static solutions: the Sandström theorem

To continue most simply, and to focus on the implications of Sandström's inference, we eliminate the salinity forcing, stress, and restoring, so that $\tau' = \gamma' = D = 0$, and assume a steady state. The only surviving non-dimensional parameter is R. T' is necessarily periodic in ϕ and so

$$\begin{aligned} T'(\phi) &= \sum_{n=-\infty}^{\infty} \alpha_n e^{in\phi}, \\ \delta(\phi - \phi_\pm) &= \frac{1}{2\pi}\sum_{n=-\infty}^{\infty} e^{in(\phi-\phi_\pm)}. \end{aligned} \tag{11}$$

Substituting into eq. (6),

$$T'(\phi) = \sum_{n=-\infty}^{\infty} \frac{e^{-in\phi_+} - e^{-in\phi_-}}{w' in + Rn^2} e^{in\phi}. \tag{12}$$

$\alpha_0 = 0$ by virtue of the zero mean value of the sources. Note that w' is still unknown, but it is a constant in ϕ, which is not true if one uses the Huang (1993) natural boundary condition. Substituting into eq. (8) and integrating around the entire loop in the steady state

$$-\int_{-\pi}^{\pi} \sum_{n=-\infty}^{\infty} \frac{e^{-in\phi_+} - e^{-in\phi_-}}{w' in + Rn^2} e^{in\phi} \sin\phi \, d\phi = 2\pi w'. \tag{13}$$

All terms except $n = \pm 1$ vanish, and eq. (13) produces

$$-w' \frac{\cos\phi_+ - \cos\phi_-}{R^2 + w'^2} + R\frac{\sin\phi_- - \sin\phi_+}{R^2 + w'^2} = w'. \tag{14}$$

Particular attention is paid here to the case in which the geopotentials of heating and cooling (and/or salt/fresh) sources are the same, $\phi_+ = -\phi_-$, intended to mimic the oceanic case. Then the Sandström theorem (e.g. Sandström, 1908; Defant, 1961; Colin

de Verdière, 1993; Munk and Wunsch, 1998; Huang, 1999; Paparella and Young, 2002) shows that the flow field should be proportional to the diffusion rates, κ_T and κ_S. Because diffusion is commonly a mechanism for dissipating structure and thus weakening flow fields, it is interesting to specifically investigate a flow that is proportional to the rate of diffusion.

The Sandström theorem asserts that, in a perfect fluid with a heating source above the cooling one, little effective work to sustain the flow against friction can be done by the buoyancy forcing alone, and that with the heating and cooling at the same level, only a very minor flow can result. ('Above' refers to the geopotential.) Although the Sandström argument is not rigorous (e.g. Paparella and Young, 2002), it does appear to have a strong qualitative validity. The situation is entirely different in the configuration – associated with Rayleigh–Bénard convection – under which the heat source lies below the cold one. Wunsch and Ferrari (2004) called the stable situation with heating above cooling 'type 2 convection', and with them at the same levels, 'type 3 convection' . The unstable (for high enough Rayleigh number) Rayleigh–Bénard situation was 'type 1' (Stern, 1975 termed types 2 and 3 'horizontal convection'). When attempting to relate the Sandström theorem to the ocean, care must be exercised because of the presence in the real system of finite external sources of mechanical energy which generate their own structures. A reinterpretation, or corollary, to the theorem would be that the observed finite abyssal stratification (finite buoyancy frequency, N) cannot be sustained by type 2 or type 3 convection in the presence of bottom water formation that would tend to fill the abyss. Instead, the external mechanical sources must provide the energy powering the turbulence inferred to mix the bottom water back to the surface. (If all deep isopycnals outcrop at the surface where direct wind-driven turbulence can provide the mixing, then no abyssal turbulent diffusion is required. The observed ocean, however, does not exhibit the required outcrops. A discussion of the upper ocean, where outcropping does exist, is quite different.)

3.1.1. Type 1 convection: heating below cooling. Suppose one heats at $\phi_+ = \pi$, and cools at $\phi_- = 0$, corresponding to Rayleigh–Bénard convection, and useful as a contrast to the type 3 situation. Then,

$$\frac{2w'}{R^2 + w'^2} = w', \tag{15}$$

whose solution is

$$w' = [0, \pm\sqrt{2 - R^2}].$$

For $R \leq 2$, the zero root corresponds to an unstable diffusive equilibrium; above $R^2 = 2$, the system is stable. The other two roots are mirror images in which $R < \sqrt{2}$; that is, the Rayleigh number must exceed $1/\sqrt{2}$ for motion to exist, otherwise the only solution is $w' = 0$. Figure 3 displays the steady-state temperature field for the case $R = 0.1$, $w' > 0$; the displaced temperature field produces the torque acting to support the flow against friction.

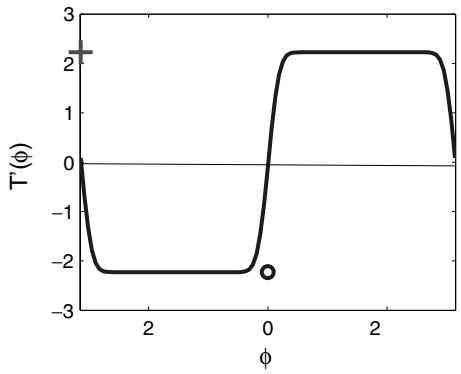

Fig 3. Temperature as a function of ϕ for $R = 0.1$, $F = 0$, and $w' > 0$, in the steady state with heating from below and cooling from above (type 1 convection). Note that the sense of ϕ has been reversed for visual convenience, with the heat source to the viewer's left. The position of the cold source is at 'o', and of the warm at '+'. The values were obtained from a 40-term sum of the Fourier series, with tapering introduced to suppress Gibbs effects.

When $R = 0$ (equivalent to zero diffusion), there is nonetheless a pair of symmetric solutions with $w' = \pm 2$, the maximum value (cf. Tritton, 1988, section 17.3).

3.1.2. Type 3 convection: heating and cooling at the same level. For an oceanic analog, the most interesting case is heating and cooling at the same level. Take $\phi_+ = -\phi_- = \pi/4$, and eq. (14) reduces to

$$(R^2 + w'^2)w' = -\sqrt{2}R \tag{16}$$

(cf. eq. 15) with one real root for $R > 0$

$$w' = \frac{1}{6}[12(162R^2 + 12R^6)^{1/2} - 108R\sqrt{2}]^{1/3} - \frac{2R^2}{[12(162R^2 + 12R^6)^{1/2} - 108R\sqrt{2}]^{1/3}}, \tag{17}$$

and plotted in Fig. 4. Note that $w' < 0$; that is, flow is from warm to cold at the top, which will be called a 'thermal' mode.

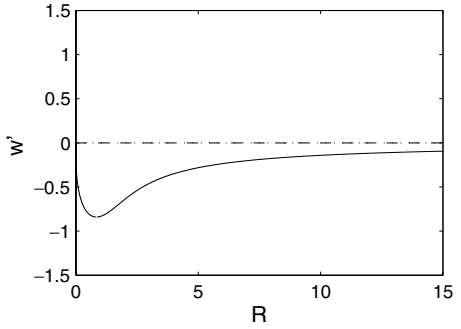

Fig 4. w' versus the inverse Rayleigh number, R, for the case in which the heat source and sink are at the same level, ($\phi_\pm = \pm\pi/4$). $w' < 0$ implying flow from the warm source toward the cold sink. R_c is defined as the value at the minimum of w'.

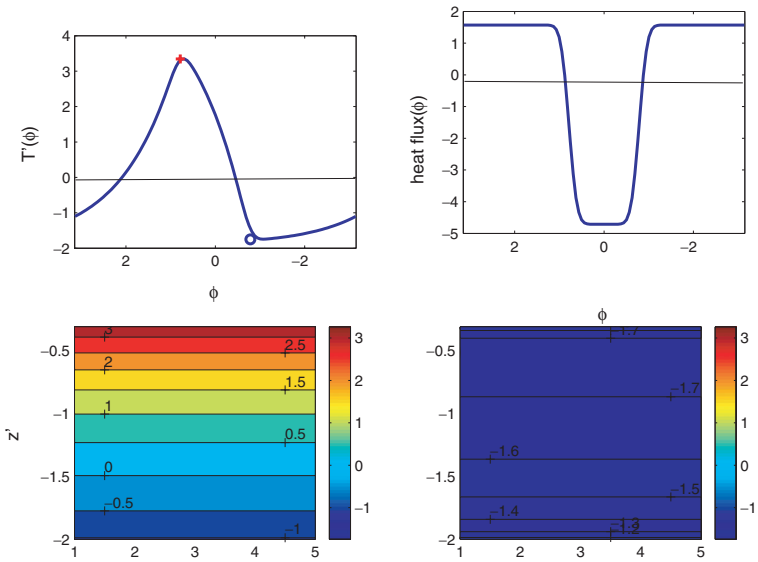

Fig 5. Type 3 convection with $w' = -0.83$ and $R = 1$. The upper-left panel shows temperature as a function of ϕ in radians (but reversed to place positive ϕ values to the left). Heat source (+) and cooling source (o) are shown at the appropriate angles. The upper-right panel is the heat flux F_H as a function of ϕ. The lower-left panel is a pseudo-subtropical box, mimicking that in S61, plotted with an arbitrarily chosen width so as to permit contouring the temperature field, with $z = -1 + \cos\phi$. This box displays upwelling of cold water in equilibrium with downward diffusion of heat. The lower-right panel is the corresponding pseudo-subpolar box. Here one has downwelling and a near-uniform temperature. The upper depth limit in the two pseudo-boxes is the depth of the sources.

There exists a maximum value of $|w'|$ (Fig. 4) and defining $R = R_c$. For small R (large Ra), eq. (17) is

$$w' \approx -2^{1/6} R^{1/3} + O(R^{5/3})$$

or $|w'| \propto k^{1/3}$, vanishing as expected, as the diffusion goes to zero (with fixed ε, this limit is one of infinite Prandtl number). The fact that there is no motion in this situation (in contrast to type 1 convection) with no diffusion is a result consistent with the Sandström theorem. As is clear from Fig. 4, the flow also vanishes as $R \to \infty$, i.e. as the diffusion grows large. Sufficiently large diffusion forces the fluid towards a more uniform temperature, and thus a weakened flow. Increasing diffusion can either strengthen or weaken the flow, depending upon the corresponding value of R relative to R_c. The temperature from a solution with $R = 0.1$ is displayed in the upper part of Fig. 5. The heat flux

$$F_H = w'T'(\phi) - R\frac{\partial T'}{\partial \phi}, \tag{18}$$

is also displayed.

Following S61, we can map the present purely thermally driven loop onto a pseudo-oceanographic form with the two regions, $-\pi \le \phi \le \phi_-$ and $\phi_+ \le \phi \le \pi$, shown as though they were polar and tropical oceanic basins, respectively (lower part of Fig. 5). For plotting purposes, the lower pipe of S61 has been reduced to an infinitesimal length, the entire region below the sources being shown as part of the two boxes, and $z' = -1 + \cos\phi$. In this configuration of relatively high diffusion, the subtropical box maintains a finite stratification in a balance between upwelling cold water and downward heat diffusion. The polar box both downwells and diffuses heat, rendering it nearly uniform below the incoming warm water.

The low diffusion limit of the loop is depicted in pseudo-oceanographic form in Fig. 6. The deeper parts of both pseudo-boxes are cold and nearly homogeneous, in the analog of the filling-box limit discussed by Munk and Wunsch (1998). The tropical box is now dominated, below the heat source, by the upwelling cold water. Homogeneous fluid can be the result of either very small or very large (as in S61) diffusion. Note that, despite the large change in the magnitude of w' (the mass flux) and in the temperature distribution, the heat flux is nearly unchanged between Figs. 5 and 6. One must carefully distinguish mass and heat flux in all such flows – the thermal and mass circulations are not the same even in this simple example (Wunsch, 2002).

3.2. *Sandström theorem and the effects of stress*

We now seek to understand the effects of a stress on the resulting flow. Stommel and Rooth (1968) modified the S61 model, omitting salinity effects, but considering the effects of a wind stress on the flow field. They concluded that in this situation, there would be two equilibria: one with a strong stress-driven flow supporting the buoyancy forcing, and the second a weak, nearly stalled flow in which the stress and buoyancy opposed each other. To explore this situation, and still without salinity effects, let $\tau' \neq 0$ in eqs. (8) and (13) reduce in the steady state to

$$-\int_{-\pi}^{\pi} \sum_{n=-\infty}^{\infty} \frac{e^{-in\phi_+} - e^{-in\phi_-}}{w'in + Rn^2} e^{in\phi} \sin\phi \, d\phi = 2\pi(w' - \tau').$$

For the case $\phi_\pm = \pm\pi/4$, this becomes

$$(R^2 + w'^2)(w' - \tau') = -\sqrt{2}R. \tag{19}$$

In one dimension, choosing values of τ' to represent an analog of the oceanic case of combined stress and buoyancy forcing is not so easy. At subtropical North Atlantic latitudes, the wind-driven interior flow combines a northward Ekman flux at the surface with a southward geostrophic flow at depth; however,

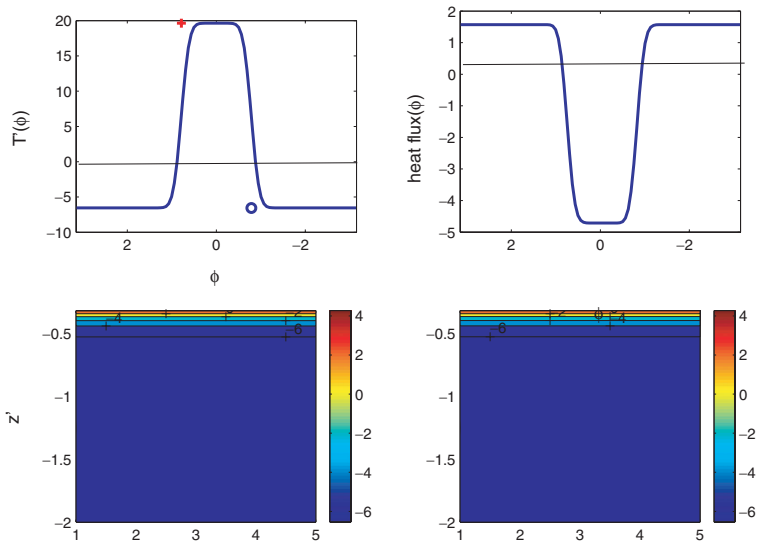

Fig 6. Same as in Fig. 5 except for $w' = -0.24$ and $R = .01$, i.e. for very small diffusion. The near homogeneity of the two pseudo-boxes displays the 'filling-box' limit discussed by Munk and Wunsch (1998). Note the heat flux at $\phi = 0$ has not changed despite the very different temperature distribution and value of w'.

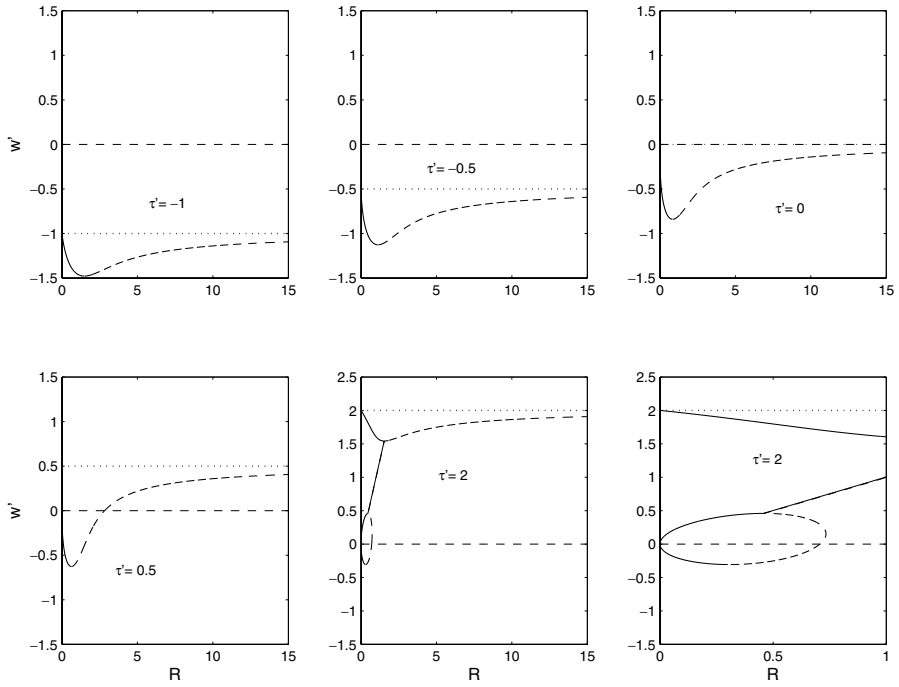

Fig 7. Roots of eq. (19) for $R(w')$ for varying values of τ'. The case $\tau' = 0$ is repeated here (see Fig. 4) for completeness. When $\tau' < 0$, the thermal driving reinforces the effects of the stress. However, when $\tau' > 0$, thermal and stress driving compete, with stress dominating for large inverse Rayleigh numbers, and with the thermal effects becoming stronger in the limit of small diffusion. The case $\tau' = 2$ is displayed twice with different axes to show the structure for small R. For large R there is only one solution, near $w' = \tau'$, but for small diffusivity, multiple roots appear. The solid line is the positive root $R(w')$ and the dashed line is the negative. The value of τ' is shown as a dotted line.

there is a southward Ekman flow in the northern part of the gyre. In bulk, however, the northward advection of warm water in the Gulf Stream system dominates the entire wind-driven system at subtropical latitudes, and leads to choosing $\tau' \leq 0$. Both the stress and thermal forcing act then to drive the surface flow from warm to cold, and eq. (19) produces $w'(R)$ which shifts quantitatively from the no-stress case, but introduces no new behavior.

In a subpolar gyre, however, one might argue that $\tau' > 0$ is physically most interesting (the difficulty of using a single-loop geometry to describe a real ocean flow is evident once again). With $\tau' > 0$, wind and thermal forcing are opposed at the surface. Equation (19) is again cubic in w', but it is quadratic in R as a function of w'. Solving for $R(w', \tau')$ leads to the results shown in Fig. 7, which includes a repetition of the case $\tau' = 0$. For

large R, that is, large diffusion, all cases asymptote near $w' = \tau'$, with the thermally driven flow systematically producing a small contribution in the negative direction. As $R \to 0$, $\tau' > 0$, $w' = 0$, is the solution. When $\tau' < 0$, the $R \to 0$ limit is $w' = \tau'$. For large positive τ' there are multiple roots at small R, some of which are spurious. The case $\tau' = 2$ is displayed in Fig. 7, showing the structure for small R. The time-dependent calculation (below) shows that the small R, low-diffusion, steady-state asymptote is $w' \to 0$. This is the Stommel and Rooth 'stalled' solution. When $\tau' = 2$, there exist multiple roots at small R (Fig. 7); which are stable and unstable remains to be determined.

For positive τ' in the small diffusion limit, one anticipates that slow temporal changes in τ' and R lead to a complex system behavior. In the interests of space, however, we turn now to the transient behavior under forcing proportional to the Heaviside function.

4. Transient behavior

Keller (1966) assumed an inertialess flow, $F \to 0$, which is a high Prandtl number limit, and for the moment, we follow that lead. Substituting into eq. (6), treating w as time-independent, and taking the Laplace transform, produces [with $T'(\phi,\ t = 0) = 0$]

$$\tilde{\alpha}_n(s) = \frac{\mathrm{e}^{-\mathrm{i}n\phi_+} - \mathrm{e}^{-\mathrm{i}n\phi_-}}{s(s + \mathrm{i}w'n + Rn^2)},$$

where the tilde represents the Laplace transform in variable s. From the inverse transform

$$\alpha_n(t') = \frac{\mathrm{e}^{-\mathrm{i}n\phi_+} - \mathrm{e}^{-\mathrm{i}n\phi_-}}{w'\mathrm{i}n + Rn^2}\left[1 - \mathrm{e}^{-(\mathrm{i}nw' + Rn^2)t'}\right].$$

Substituting into the reduced form of eq. (8), and integrating over the loop, again only the $n = \pm 1$ terms will survive the integration producing

$$\begin{aligned} -\int_{-\pi}^{\pi} & \frac{\mathrm{e}^{-\mathrm{i}\phi_+} - \mathrm{e}^{-\mathrm{i}\phi_-}}{w'\mathrm{i} + R}\left[1 - \mathrm{e}^{-(\mathrm{i}w' + R)t'}\right]\mathrm{e}^{\mathrm{i}\phi}\sin\phi\,\mathrm{d}\phi \\ & - \int_{-\pi}^{\pi} \frac{\mathrm{e}^{\mathrm{i}\phi_+} - \mathrm{e}^{\mathrm{i}\phi_-}}{-w'\mathrm{i} + R}\left[1 - \mathrm{e}^{-(-\mathrm{i}w' + R)t'}\right]\mathrm{e}^{-\mathrm{i}\phi}\sin\phi\,\mathrm{d}\phi \cdot \\ & = 2\pi w'(t') \end{aligned} \tag{20}$$

w' is always real, and $T'(\phi)$ is stable for all $R > 0$. One must verify, after the fact, that the solution for w' satisfying eq. (13) does not violate the assumption that $F\,\mathrm{d}w'/\mathrm{d}t'$ is negligible.

4.1. Type 1 convection

With $\phi_+ = \pi$, $\phi_- = 0$, the solution is

$$T'(\phi, t') = 2\mathrm{Re} \times \left\{\sum_{n=1}^{\infty}(\mathrm{e}^{-\mathrm{i}n\pi} - 1)\frac{\left[1 - \mathrm{e}^{-(\mathrm{i}nw' + Rn^2)t'}\right]}{\mathrm{i}w'n + n^2R}\mathrm{e}^{\mathrm{i}n\phi}\right\} \tag{21}$$

with

$$\begin{aligned} \mathcal{F} \doteq & \frac{2}{w'^2 + R^2} \\ & \times (-w' - R\mathrm{e}^{-Rt'}\sin w't' + w'\mathrm{e}^{-Rt'}\cos w't') \\ & + w' = 0 \end{aligned} \tag{22}$$

from eq. (20) determining $w'(t')$. Equation (22) reduces to eq. (15) as $R \to \infty$. If $\mathcal{F}$ is contoured as a function of w' (not shown), the zero contours define the values of $w'(t')$ in eq. (21). There are two symmetric roots $\pm w'$, and the multivaluedness for about $t' < 20$ leads to abrupt oscillations corresponding to the motions described by Keller (1966). Although formally acceptable for $F = 0$, the discontinuities violate the assumption that $F\,\mathrm{d}w'/\mathrm{d}t' \approx 0$, for small F, and the physical validity of this solution is doubtful; however, they are strong evidence that oscillations are to be expected.

We resort to direct numerical integration. Substituting the Fourier series (11) into eq. (6) requires for $\alpha_{\pm 1}$

$$\frac{\mathrm{d}\alpha_1(t')}{\mathrm{d}t} = [-\mathrm{i}w'(t') - R]\alpha_1(t') + \exp(-\mathrm{i}\phi_+) - \exp(-\mathrm{i}\phi_-) \tag{23}$$

$$\frac{\mathrm{d}\alpha_{-1}(t')}{\mathrm{d}t} = [\mathrm{i}w'(t') - R]\alpha_{-1}(t') + \exp(\mathrm{i}\phi_+) - \exp(\mathrm{i}\phi_-), \tag{24}$$

and the integrated form of eq. (8) is

$$2\pi F\frac{\mathrm{d}w'(t)}{\mathrm{d}t'} + \mathrm{i}[\alpha_1(t) - \alpha_{-1}(t)]/2 - 2\pi w'(t) = 0. \tag{25}$$

Following Malkus (1972), and writing $\alpha_1 = a_1 + \mathrm{i}b_1$, $\phi_+ = \pi$, one readily finds that the equations governing $\mathrm{d}a_1/\mathrm{d}t'$, $\mathrm{d}b_1/\mathrm{d}t'$, and $\mathrm{d}w'/\mathrm{d}t'$ are those of Lorenz (1963) in the chaotic regime; here, w' corresponds to the X variable. Tritton (1988, pp. 246–254) has a nice account of this work, and also see Creveling et al., (1975), Hart (1984), Erhard and Müller (1990), Wang et al., (1992), and Dewar and Huang (1995) among others. Thus, this simple loop, with thermal forcing alone, exhibits all the richness of the Lorenz system. As this regime has been well explored, we will not dwell on it here. The asymptotic steady states of the $F \neq 0$ regime are the same as described above for $F = 0$. [The use of heat sources in the present configuration, as opposed to an imposed thermal boundary condition, puts a forcing term into the Lorenz X equation, but the qualitative nature of the solutions is unchanged. Palmer (1999) discusses some aspects of the forced Lorenz system.]

The type 1 configuration has no direct oceanographic application, apart from geothermal heating, but serves as a contrast to the type 3 convective example below. A marginal type 1 application would include the case in which solar heating penetrates significantly below the sea surface, with ocean cooling being confined to the surface. Geothermal heating contributes only modestly to the ocean circulation (e.g. Adcroft et al., 2001), and we turn now to the more important type 3 case.

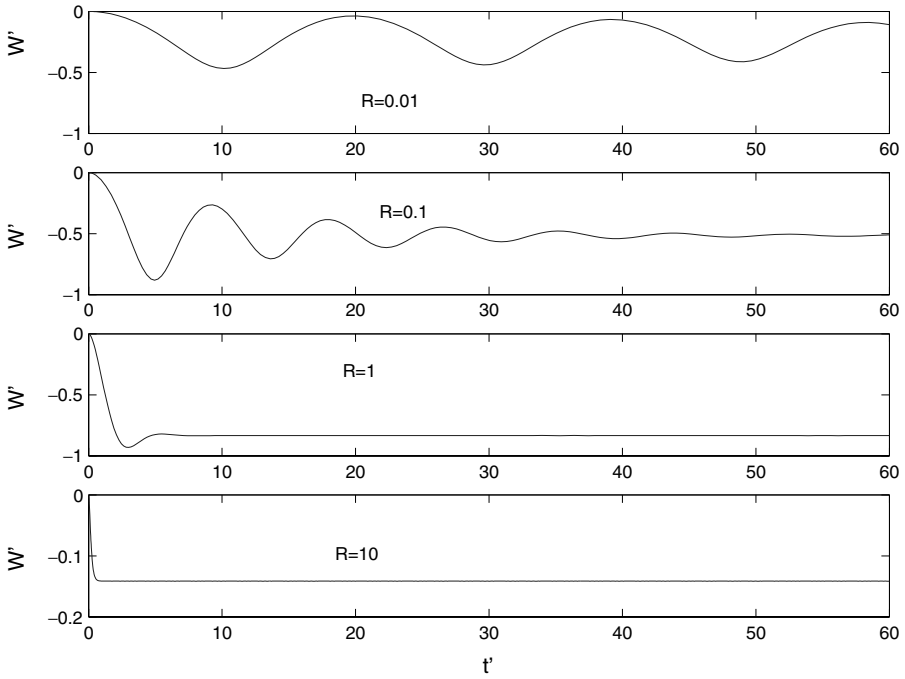

Fig 8. Temporal behavior of the solutions, started from rest, under purely thermal driving. $Pr = 1$, for varying values of R. The ultimate asymptote is always to a purely thermal, steady, mode. Note the vertical scale change.

4.2. Type 3 convection

Four solutions for different values of R are shown, for $Pr = 1$, in Fig. 8, when started from $w' = 0$. These figures are typical of many further examples (not shown) for varying Pr and R, and simply demonstrate that in type 3 convection, the steady states can be reached via oscillatory or heavily damped behavior. Unlike type 1 convection, there is no chaotic regime and the motions become steady for the entire parameter range with a stable fixed point in the thermal mode.

When stress is introduced, the equation governing the transient behavior of the thermal/stress system of the last section is

$$2\pi F \frac{\mathrm{d}w'}{\mathrm{d}t'} + \mathrm{i}[\alpha_1(t') - \alpha_{-1}(t')]/2 - 2\pi(w' - \tau') = 0, \qquad (26)$$

along with eqs. (23) and (24). Negative τ' values simply reinforce the thermal mode. The most interesting case is for moderate (relative to R) positive values of τ'. For the case $\tau' = 2$ in Fig. 7, the transient behavior, starting with both $w'(0) = \tau'$ and $w'(0) = 0$, is displayed in Figs. 9 and 10, with $Pr = 100$. The low R solutions oscillate, eventually converging to the small w' roots in Fig. 7 of the stalled mode. For sufficiently large R, however, the asymptote is always in the stress mode, with $w' \approx \tau'$. The importance of stress in determining the nature of the flow is evident.

5. Salinity, and temperature with restoring

S61 considered the situation in which both temperature and salt driving through relaxation boundary conditions were present, but not stress. Stommel identified the two steady states possible: a thermal mode with comparatively rapid flow at the top from warm to cold, and the reversed 'salinity mode' from cold to warm. In the present configuration, we can readily explore a very large range of conditions in the loop, including the addition of salt sources with and without stress, restoring in temperature or salinity or both with a variety of time-scales, parameter ranges, and time history of the sources. The range of behavior of the loops, with so many non-dimensional parameters, and accounting for all of the possible transient behaviors, is very large, and perhaps enlightening only in the existence of this intricacy. Although a number of calculations were made of steady and transient behavior in the presence of heat and salt sources, these will be omitted here. We turn instead to the configurations involving heat and salt sources, temperature restoring, and stress – primarily to suggest the fragility of any inference about analogs between GCMs and any particular parameter range of the loops.

The most common studies of systems such as these (including S61) has been in the context of temperature boundary conditions involving restoring to some form of climatology, either to mimic a simple atmospheric feedback, or to force the system to be more realistic if it drifts away under pure thermal flux boundary conditions. With $\tau' = 0$, in the absence of restoring terms, there is only one solution type, as the co-located temperature and salinity sources combine to produce a net density source. Rather than reproduce the S61 situation with restoring in both temperature and salinity and no sources, the sources are retained here, and salinity is left without restoring, giving 'mixed' boundary conditions (and the reader is reminded of the conclusions of Huang,

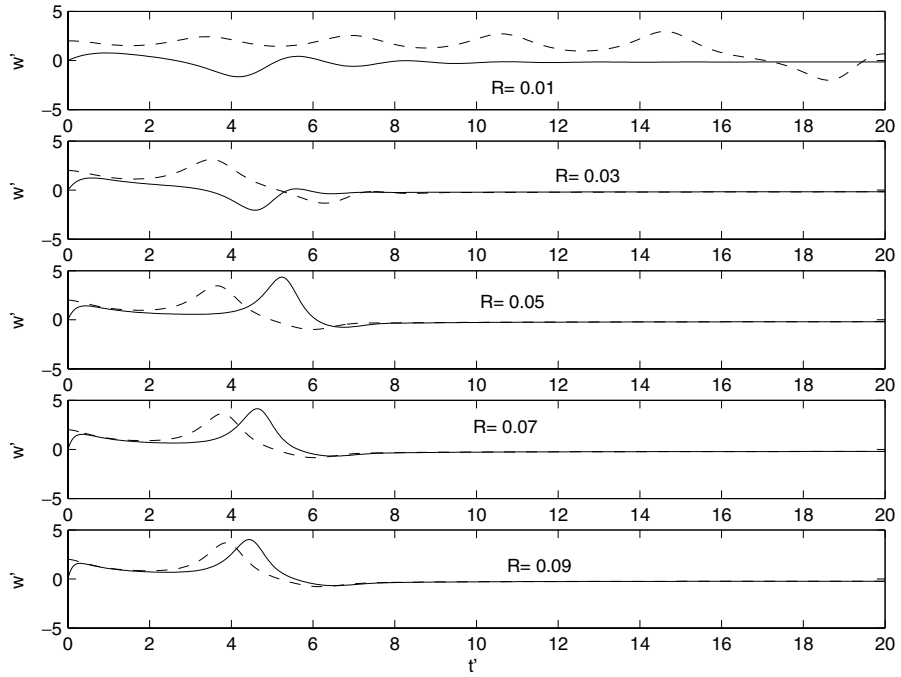

Fig 9. Type 3 convection, with temperature forcing and $\tau' = 2$. $Pr = 100$ in all cases, for varying values of R. Each panel, for fixed R, shows the solutions when the initial condition is $w'(0) = 0$ (solid), and the dashed line when $w'(0) = \tau'$. For sufficiently small R both solutions converge to the stalled mode, but if started in the stress mode, oscillations about the stress mode occur prior to the transition.

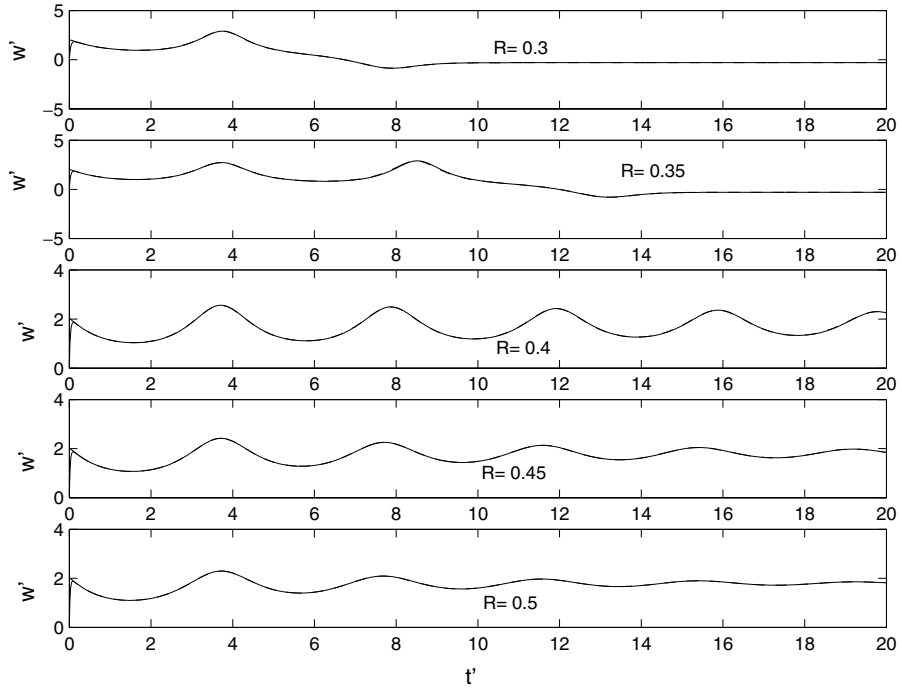

Fig 10. Same as Fig. 9, except for larger values of R. The solutions from the two different starting initial conditions converge almost immediately, and essentially invisibly here. However, for small R, the convergence is to the stalled mode, and for large R it is to the stress mode. Note the change in vertical scale.

1993 concerning the importance of natural boundary conditions on salt, i.e. for mass). The steady-state direction of flow will be determined by the stronger of the heat and salt sources. More generally, the presence of restoring produces a system energetics that is very difficult to understand (taken up below), and how seriously any of these solutions should be regarded is very unclear. We proceed, none the less.

Let the restoring terms in eq. (6) include $T^{*'}$ defined as

$$T^{*'}(\phi) = \sum_{n=-\infty}^{\infty} \delta_n e^{in\phi}, \delta_0 = 0, \tag{27}$$

where only $\delta_{\pm 1}$ will affect the flow rate, w'. (Other terms determine the temperature distribution within the loop.) We will take $\delta_{\pm 1} = \pm 1/2i$. With restoring, the Sandström theorem cannot be invoked until the solution is found, as buoyancy can be provided at all depths, depending in part on the actual flow and temperature fields established. For salinity, we define a new Fourier series

$$S'(\phi) = \sum_{n=-\infty}^{\infty} \beta_n e^{in\phi}.$$

5.1. Steady states

In the steady state, the Fourier coefficients for the temperature perturbation are now

$$\alpha_n = \frac{e^{-in\phi_+} - e^{-in\phi_-} + \gamma' \delta_n}{w' in + Rn^2 + \gamma'} \tag{28}$$

and those for salinity are

$$\beta_n = \frac{-e^{-in\phi_+} + e^{-in\phi_-}}{w' in + R_S n^2}.$$

Assume, for simplicity, that $R_S = R_T = R$. (We can readily explore the situation when heat and salt are diffused at different rates, but that analysis is omitted.) Then substituting into eq. (8) and integrating around the loop produces

$$-\frac{1}{2}\frac{2\sqrt{2}(R+\gamma') + R\gamma' + \gamma'^2}{(R+\gamma')^2 + w'^2} + D\frac{\sqrt{2}R}{R^2 + w'^2} - w' + \tau' = 0, \tag{29}$$

which is a quintic for $w'(R)$ or cubic for $R(w')$. Consider first $\gamma' = 1$, $\tau' = 0$, $D = 1$. The real roots $w'(R')$ are displayed in Fig. 11. For large R, there is a weak thermal mode, but for small R, three roots appear: strong and weak thermal modes as well as a weak salinity mode. The latter persists until a transition takes place to the high R thermal mode. The stability of these roots can be investigated by the usual formal methods for analysis of nonlinear systems, but given the issues of realism already raised, we will not pursue the subject here. Fig. 12 shows the three real roots of the polynomial as a function of R for $\tau' = -1$, $\gamma' = 1$, and $D = 1$. With $D = 1$, the salt and heat sources cancel locally in the equation of state; however, because restoring is applied only to the temperature component of density, the salinity field still influences the flow.

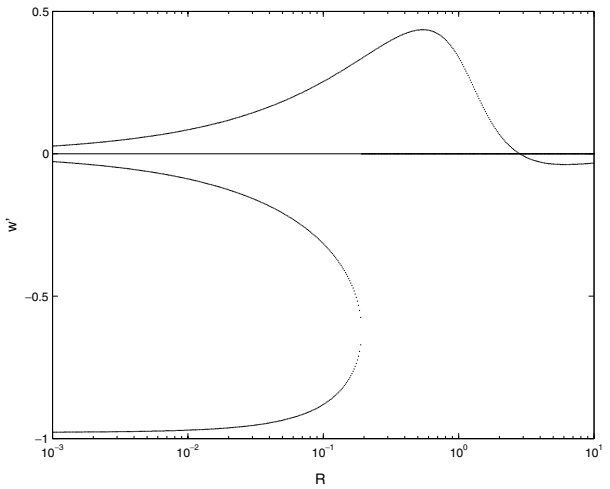

Fig 11. Roots of the quintic eq. (29) with $\tau' = 0$, and $\gamma' = 1$. Stability of these roots varies with Pr.

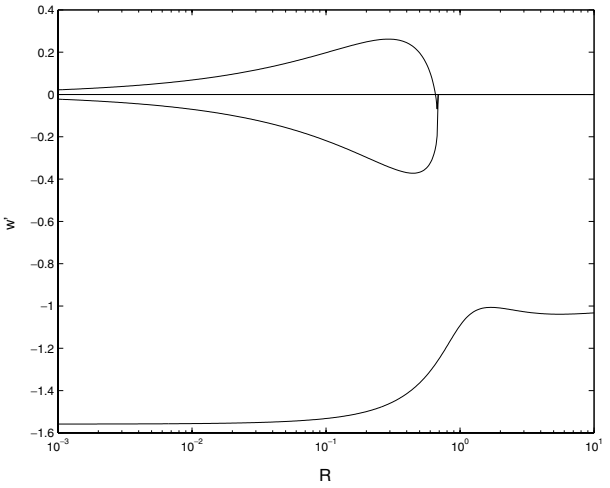

Fig 12. $w'(R)$ for $\tau' = -1$, $\gamma' = 1$, temperature with restoring and $R_S = R$. The precise value of R (diffusion) evidently can make a large difference to the nature of the solution. The stress attempts to drive a thermal mode but can be overcome, at sufficiently small diffusion, by the salinity forcing.

When $\tau' = -1$ (Fig. 12), for large R there is only one root, while for small R there are three roots. Thermal and salinity modes correspond to w' less than or greater than zero, respectively. Two roots exist for the thermal mode and one for salinity. The salinity mode is a near mirror image of the weak thermal mode; the latter is not realizable (it is unstable). When $\tau' = 2$, this situation produces three thermal modes at low R, but only a single one at large R, asymptoting to $w' = \tau'$ with R (not shown).

In this restoring system, the steady-state asymptotes are no longer independent of Pr or F. The value of Pr determines which asymptotic branch of Fig. 12 is reached for small values of γ'. For small γ', there clearly is considerable sensitivity of the

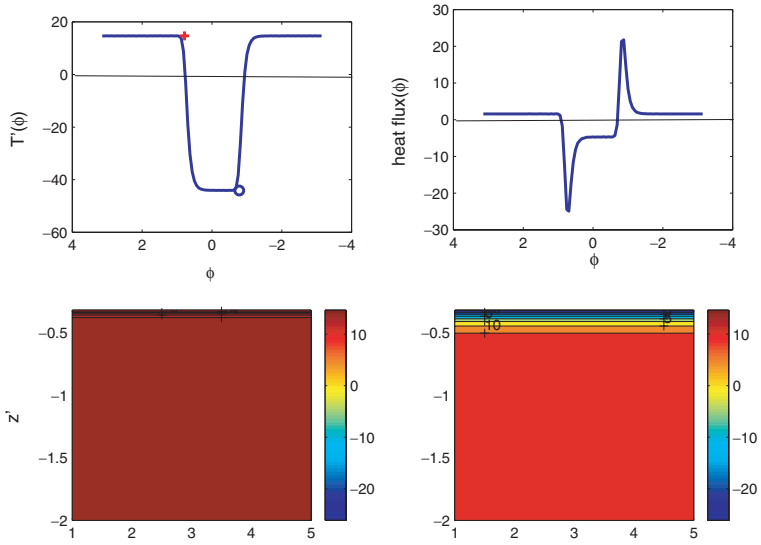

Fig 13. Steady-state temperature distribution of the asymptotic value of the salinity mode of Fig. 12. The warm abyssal ocean contrasts with the thermal mode solutions. $w' = 0.11$, $D = 1$, $\gamma' = 1$, and $R = 0.1$.

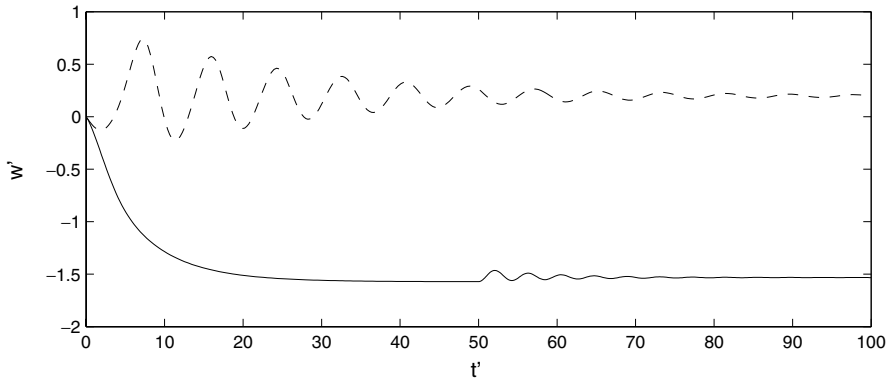

Fig 14. Comparison of delayed onset of haline forcing. The dashed curve shows the temporal response when both heat/salt sources are turned on at $t' = 0$, with $R = 0.1$, $\tau' = -1$, and $Pr = 1$. The solid curve is the response when the salt source onset is delayed until $t' = 50$. Without delayed onset, the system oscillates and ultimately settles into a salinity mode, while delayed onset leads to a stable thermal mode.

transient behavior as a function of γ'. The steady-state asymptotic temperature distribution of the salinity mode at $Pr = 10$ (independent of γ) is shown in Fig. 13. The temperature and heat flux distributions are very different from those in the thermal modes (not shown).

The main message here is that an intricate set of behaviors is possible, dependent in large part on the presence of temperature restoring, but also on the magnitude and direction of τ'. Temporal behavior is a sensitive function of the non-dimensional parameters and given the great difficulty in interpreting them in a three-dimensional context, we will now turn to one last configuration.

5.2. *Delayed onset of haline forcing*

Because of the widespread inference that the introduction of fresh water into a North Atlantic-like system dominated by a thermal mode can convert it abruptly into a reversed salinity mode, with all its climate consequences, it is interesting to briefly consider the way in which the loop models respond to the abrupt switching on of a high-latitude freshening, and a low-level salinity increase. We have already seen that for small R and $\tau' \neq 0$, oscillatory states are possible. Not surprisingly, within such states, one can have a very different outcome depending upon where in the oscillation cycle the salinity forcing occurs.

The introduction of haline forcing into the time-dependent system can be anticipated to introduce yet another parameter, and many earlier results with GCMs show that the history of the flow in part determines the result of the sudden onset of a freshwater source. To depict this behavior in a single example, Fig. 14 shows the case, $\tau' = -1$, $\gamma' = 1$, $Pr = 1$, $R = 0.1$, when the salinity sources are turned on at $t' = 0$, with the system at rest, and when their onset is delayed until $t' = 50$, at a time when the flow has already settled down into a stable thermal mode. In the first instance, the system oscillates before ultimately settling into a weak salinity mode. With a delayed onset, there is a minor

oscillation about the thermal mode, but no major change other than an eventual slight weakening of the thermal mode state. Depending upon precise parameter values, including the time of onset, t_c, a great variety of behaviors is possible. (For example, if $\tau' = 1$, choosing $t'_c = 50$ does force the system to jump into the haline mode.) In general, at low R, one anticipates the existence of hysteresis effects from cycling boundary conditions, but these effects, too, are omitted here.

Unless one were convinced of the ability to connect both the parameter ranges and the actual physical behaviors of the loop models with those in GCMs, there appears to be little oceanographic or climatic point in proliferating examples of this type. They are undoubtedly of interest in their own right.

6. Energetics

A considerable recent literature has collected around the question of which external forces provide the energy to sustain the ocean circulation (reviewed by Wunsch and Ferrari, 2004), and resulting in the conclusion that only wind and tides are significant. Because that inference has important implications for the behavior of the climate system, it is thus useful to briefly consider the energetics of the loops – if they are intended as surrogates for the ocean.

Consider thermal and stress forcing alone ($D = S_0 = 0$). Multiply eq. (8) by w' for a dimensionless kinetic energy equation

$$F\frac{\partial}{\partial t'}\left(\frac{w'^2}{2}\right) = -\frac{\partial p'}{\partial \phi}w' + w'\sin\phi - w'T'(\phi)\sin\phi - w'^2 + \tau' w',$$

which, when integrated over the loop, produces

$$F\frac{\partial}{\partial t'}\int_{-\pi}^{\pi}\frac{w'^2}{2}\mathrm{d}\phi = -w'\int_{-\pi}^{\pi}T'(\phi)\sin\phi\,\mathrm{d}\phi + 2\pi\tau' w' - 2\pi w'^2, \tag{30}$$

with stress providing the only external direct source term. A nondimensional potential energy equation is obtained by multiplying the negative of eq. (6) by $z' = -1 + \cos\phi$ and integrating over the loop. Integrating by parts where appropriate gives

$$\frac{\partial}{\partial t'}\left[-\int_{-\pi}^{\pi}\cos\phi T'(\phi)\,\mathrm{d}\phi\right] = w'\int_{-\pi}^{\pi}\sin\phi T'(\phi)\,\mathrm{d}\phi + R\int_{-\pi}^{\pi}\cos\phi T'(\phi)\,\mathrm{d}\phi - \gamma'\int_{-\pi}^{\pi}[T^*(\phi) - T'(\phi)]\cos\phi\,\mathrm{d}\phi - 2\pi(\cos\phi_+ - \cos\phi_-). \tag{31}$$

Notice (e.g. Wunsch and Ferrari, 2004) that the term

$$w'\int_{-\pi}^{\pi}\sin\phi T'(\phi)\,\mathrm{d}\phi,$$

occurs with opposite sign in the kinetic and potential energy equations, and that its contribution to the total energy vanishes. It represents the conversion term between potential and kinetic energies and it can operate in either direction.

Suppose first that $\gamma' = 0$. The last term in eq. (31) represents the direct potential energy production by the sources. For type 1 convection, $\phi_+ > -\phi_-$, the contribution to the potential energy is positive. In type 2 convection, $\phi_+ < -\phi_-$ and the sources decrease the potential energy. If $\phi_+ = -\phi_-$, in type 3, this source term vanishes, and there is no generation of potential energy by external forcing. The balance then is between the conversion from kinetic energy and its removal by diffusion.

Because

$$\frac{\partial}{\partial t}\int_{-\pi}^{\pi}T'(\phi)\,\mathrm{d}\phi = 0,$$

there is no net generation of internal energy.

In a steady state, we have the balance of kinetic energy

$$-w'\int_{-\pi}^{\pi}\sin\phi T'(\phi)\,\mathrm{d}\phi + 2\pi\tau' w' = 2\pi w'^2, \tag{32}$$

of potential energy

$$w'\int_{-\pi}^{\pi}\sin\phi T'(\phi)\,\mathrm{d}\phi = -R\int_{-\pi}^{\pi}\cos\phi T'(\phi)\,\mathrm{d}\phi, \tag{33}$$

and of total energy

$$2\pi\tau' w' = 2\pi w'^2 - R\int_{-\pi}^{\pi}\cos\phi T'(\phi)\,\mathrm{d}\phi. \tag{34}$$

When $\tau' = 0$, the only way to provide an energy source to balance the frictional dissipation term, $2\pi w'^2$, is by the generation of potential energy from diffusion, consistent with the Sandström theorem. Diffusion, as has already been seen, can act either to increase or to reduce the flow, depending upon the sign of $\cos\phi T'(\phi)$, that is, determined by its mean behavior above and below the center line, $\phi = \pm\pi/2$.

Equation (34) suggests a possible parametrization of diffusion in terms of stress. If it is assumed that the mechanical dissipation in the system remains fixed as in Huang (1999) – the justification for this assumption is not very clear, but neither is the usual alternative of constancy of $\kappa_{T,S}$ – assuming $\kappa_T = \kappa_S = \kappa$, we have

$$2\pi\tau' w' + R[\kappa(\tau')]\int_{-\pi}^{\pi}\cos\phi T'(\phi)\,\mathrm{d}\phi = \text{constant}. \tag{35}$$

More generally, ocean models need to begin the parametrization of mixing coefficients as functions of the externally applied mechanical driving, $\kappa(\tau', \eta)$, where η represents tidal amplitudes and mixing (see, for example, Wunsch and Ferrari, 2004), which are in turn functions of the oceanic geographic configuration. The nature of this parametrization is the focus of much ongoing work (e.g. Jayne and St. Laurent, 2001). Discussions of mixing parametrized in terms of wind stress can be found in Oberhuber (1993) and McDougall and Dewar (1998).

When temperature restoring is reintroduced, the energy discussion becomes more complicated. For type 3 convection,

eq. (31) is

$$\frac{\partial}{\partial t}\left[-\int_{-\pi}^{\pi}\cos\phi T'(\phi)\,\mathrm{d}\phi\right] = w'\int_{-\pi}^{\pi}\sin\phi T'(\phi)\,\mathrm{d}\phi - (R+\gamma')\int_{-\pi}^{\pi}\cos\phi T'(\phi)\,\mathrm{d}\phi - \gamma'\int_{-\pi}^{\pi}\cos\phi T'^{*}(\phi)\,\mathrm{d}\phi,$$

and the total energy balance is

$$\frac{\partial}{\partial t'}\left[-\int_{-\pi}^{\pi}\cos\phi T'(\phi)\,\mathrm{d}\phi + F\int_{-\pi}^{\pi}\frac{w'^2}{2}\,\mathrm{d}\phi\right] = (R+\gamma') \times \int_{-\pi}^{\pi}\cos\phi T'(\phi)\,\mathrm{d}\phi + \gamma'\int_{-\pi}^{\pi}\cos\phi T'^{*}(\phi)\,\mathrm{d}\phi + 2\pi\tau' w' - 2\pi w'^2. \quad (36)$$

The externally imposed temperature, T'^{*}, can be a potential (and total) energy source or sink, again depending upon its behavior relative to the horizontal center line. Imposed average warm temperatures, T'^{*}, above the center line, increase the potential energy, while negative ones decrease it. The component of T'^{*} proportional to $\sin\phi$ that contributes to the torque contributes nothing to the potential energy. In the steady state, total energy balance is

$$2\pi\tau' w' - \gamma'\int_{-\pi}^{\pi}\cos\phi T'^{*}(\phi)\,\mathrm{d}\phi = -(R+\gamma') \times \int_{-\pi}^{\pi}\cos\phi T'(\phi)\,\mathrm{d}\phi + 2\pi w'^2,$$

and restoring in general has a complicated influence on the energy budget – introducing a physical balance not possible with sources. As demonstrated by the explicit solutions above, the precise form of restoring in nature, and its numerical magnitude, can greatly affect the possible modes of flow; consequently, the physical basis for the introduction of this extra energy source/sink needs to be carefully justified. As we have seen with compensating temperature and salinity forcing, the existence of a flow in the absence of stress depends completely upon the non-zero restoring. Its energetics are obscure.

The simple conclusions possible here are that in type 3 convection characteristic of the ocean, and in the absence of stress forcing, the entire motion derives its energy from diffusion. If diffusion is molecular, the ultimate source is the internal energy at the molecular level. If diffusion derives from a parametrized turbulence, then there is a hidden external source of energy driving that turbulence, and the system is not closed. Restoring introduces another covert energy source whose magnitude and sign are difficult to determine without solving the problem completely.

7. Analogs in three dimensions?

Many additional complications can be introduced into the loop geometry. One of the more physically plausible ones consists of permitting a throughflow (Mertol et al., 1981), that tends to stabilize the flow, and which perhaps is an analog of an oceanic interbasin exchange. However, a point of diminishing returns has probably been reached.

The question of the extent to which S61-like solutions are seen in more complex flows has been discussed by Thual and McWilliams (1992) for a non-rotating two-dimensional model, and by Cessi and Young (1992) in a discussion of the former paper. The latter authors used a perturbation expansion in the vertical aspect ratio, for the high diffusion limit ('amplitude equation' approach). Cessi and Young (1992) successfully identify multiple stable states in their approximate solution corresponding to those appearing in the Thual and McWilliams (1992) full equation solution, and further identify them with the S61 states. The extension of this study to three dimensions does not appear to have been undertaken yet, and may not be possible. [In general, there appears to be little guidance available in the fluid dynamical literature concerning the relationship between one- and two-dimensional, or two- and three-dimensional (in space) flows. A limited exception is the Squire theorem (e.g. Kundu, 1990, p. 389) for shear flows, showing that there is no three-dimensional disturbance more unstable than the most unstable two-dimensional one, and hence that the stability analysis can be confined to two dimensions.] Arguments attempting to construct analogies between two- and three-dimensional systems have been given, for example, by Thual and McWilliams (1992) and Wright et al. (1998). Dijkstra and Weijer (2003) show some similarity between low-dimensional models and the bifurcations of a limited region 4° resolution GCM; numerous differences and exceptions do however occur, and such models do not resolve the very important boundary currents of the ocean.

Given the intricate behavior of the loop, and its dependence not only upon R_T, R_S, and F, but also upon D, τ', γ', and t'_c, the ability to identify any particular instability, oscillation, or bifurcation in a GCM (which will have many more parameters and three space dimensions, and hence enormously more degrees of freedom of movement) could only be done at the expense of a very long and careful analysis. The much larger number of kinematic and dynamical pathways available in a three-dimensional rotating flow relative to any one- or two-dimensional representation suggests that bifurcations, time histories, and response to external disturbances, in general, may be very different. Type 3 convective loops or the loop–Stommel box model special case are best considered as metaphors for the circulation, not as the circulation itself. Many, but far from all, of the same operative controls are present, but in the absence in the loops or box models of the complex pathways available to the general circulation, and because of the great parameter sensitivity manifested in this one-dimensional case, any inference of like-behavior should be regarded warily. Whether the motions in the two different dimensions are truly analogs of each other remains undemonstrated, and a certain skepticism should be retained.

Maas (1994) has taken a different approach to producing an internally consistent model representing S61. For a non-rotating or f-plane ocean, he writes equations for the integrated angular

momentum balance under a wind-stress torque, and for the net meridional density gradient with temperature restoring. When f vanishes, he recovers the Lorenz system; with $f \neq 0$, but with some further approximation, his system reduces to that of Lorenz (1990). Much of the behavior he deduces, with no salinity forcing, is consistent with that seen here. However, we remain far from a system with, for example, the critical effects of $\mathrm{d}f/\mathrm{d}y$ producing boundary currents and the geostrophic vorticity balance that appears so fundamental to the actual ocean circulation.

A freshwater cap on the North Atlantic is widely accepted as the most direct means of reducing the meridional mass overturning, as discussed recently by Manabe and Stouffer (1999), Wunsch (2002), and Nilsson et al. (2003) among many others. In numerous papers, the S61 model is used to rationalize the response of GCMs. In the absence of an analysis showing a deduced connection between the structure and stability of a three-dimensional flow and that appearing in the one-dimensional loops, great care needs to be exercised in analogizing the former by the latter, especially when concerned with the response to external disturbances.

8. Summary

The one-dimensional loop geometry lends itself to the production of a simple example of the implications of the Sandström theorem. When used with pseudo-salinity boundary conditions, it can mimic the behavior of the S61 and Stommel and Rooth (1968) box model, which is itself a form of loop model, albeit with an awkward specification of infinite and zero mixing rates. The loop geometry exhibits delicate dependences upon numerous non-dimensional parameters, both in its mean and transient states. Much of the appeal of loops and box models has been the supposition that they are at least qualitative, and perhaps quantitative, representations of far more complex higher-dimensional systems. The number of degrees of freedom in a three-dimensional model, even in a laminar regime is, however, orders of magnitude greater than in a one-dimensional fluid. A general theory permitting construction of correspondences between GCM non-dimensional parameter ranges and flow elements, and those in one dimension, would obviously be highly welcome, if such correspondences are possible. Low-dimensional non-linear systems frequently produce more exciting behavior than highly multidimensional systems like a GCM. Whether existing GCMs are themselves any more than a rough metaphor for the actual circulation is another open question.

9. Acknowledgment

The author acknowledges very useful comments from W. Young, S. Yuan, R. Ferrari, O. Marchal, A. Adcroft, J. Pedlosky, P. Huybers, and an anonymous referee. This work is supported in part by the National Ocean Partnership Program (NOPP) under the ECCO Consortium.

References

Adcroft, A., Scott, J. R. and Marotzke, J. 2001. Impact of geothermal heating on the global ocean circulation. *Geophys. Res. Lett.* **28**, 1735–1738.

Cessi, P. and Young, W. R. 1992. Multiple equilibria in two-dimensional thermohaline circulation. *J. Fluid Mech.* **241**, 291–309.

Colin de Verdière, A. 1993. On the oceanic thermohaline circulation. In: *Modelling Oceanic Climate Intereactions* (eds J. Willebrand, and D. L. T. Anderson). Springer-Verlag, Berlin, 151–184.

Creveling, H. F., de Paz, J. F., Baladi J. Y. and Schoenhals, R. J. 1975. Stability characteristics of a single-phase free convection loop. *J. Fluid Mech.* **67**, 65–84.

Defant, A. 1961. *Physical Oceanography*, Vol. 1. Pergamon, New York, 598 pp.

Dewar, W. K. and Huang, R. X. 1995. On the forced flow of salty water in a loop. *Phys. Fluids* **8**, 954–970.

Dijkstra, H. A. and Weijer, W. 2003. The connection of equilibria within a hierarchy of models. *J. Mar. Res.* **61**, 725–744.

Erhard, P. and Müller, U. 1990. Dynamical behavior of natural convection in a single-phase loop. *J. Fluid Mech.* **217**, 487–518.

Hart, J. E. 1984. A new analysis of the closed loop thermosyphon. *Int. J. Heat Mass Transf.* **27**, 125–136.

Huang, R. X. 1993. Real freshwater flux as a natural boundary condition for the salinity balance and thermohaline circulation forced by evaporation and precipitation. *J. Phys. Oceanogr.* **23**, 2428–2446.

Huang, R. X. 1999. Mixing and energetics of the oceanic thermohaline circulation. *J. Phys. Oceanogr.* **29**, 727–746.

Huang, R. X. and Dewar, W. K. 1996. Haline circulation: bifurcation and chaos. *J. Phys. Oceanogr.* **26**, 2093–2106.

Jayne, S. R. and St. Laurent, L. C. 2001. Parametrizing tidal dissipation over rough topography. *Geophys. Res. Lett.* **28**, 811–814.

Jeffreys, H. W. 1925. On fluid motions produced by differences of temperature and humidity. *Q. J. R. Meteorol. Soc.* **51**, 347–356.

Jiang, Y. Y. and Shoji, M. 2003. Spatial and temporal instabilities of in a natural circulation loop: influences of thermal boundary conditions. *J. Heat Transfer, Trans. ASME* **125**, 612–623.

Keller, J. B. 1966. Periodic oscillations in a model of thermal convection. *J. Fluid Mech.* **26**, 599–606.

Kundu, P. K. 1990. *Fluid Mechanics.* Academic, San Diego, 638 pp.

Lorenz, E. N. 1963. Deterministic non-periodic flow. *J. Atmos. Sci.* **20**, 130–141.

Lorenz, E. N. 1990. Can chaos and intransitivity lead to interannual variability? *Tellus* **42A**, 378–389.

Maas, L. R. M., 1994. A simple model for the three-dimensional, thermally and wind-driven ocean circulation. *Tellus* **46A**, 671–680.

McDougall, T. J. and Dewar, W. K. 1998. Vertical mixing and cabbeling in layered models. *J. Phys. Oceanogr.* **28**, 1458–1480.

Malkus, W. V. R. 1972. Non-periodic convection at high and low Prandtl number. *Mém. Soc. Royale des Sciences de Liège*, 6th série, tome IV, 125–128.

Manabe, S. and Stouffer, R. J. 1999. Are two modes of thermohaline circulation stable? *Tellus* **51A**, 400–411.

Marotzke, J. 2000. Abrupt climate change and thermohaline circulation: Mechanisms and predictability. *Proc. Natl. Acad. US.* **97**, 1347–1350.

Mertol, A., Greif, R. and Zvirin, Y. 1981. The transient, steady state and stability behavior of a thermosyphon with throughflow. *Int. J. Mass Heat Transfer* **24**, 621–633.

Munk, W. and Wunsch, C. 1998. Abyssal recipes II: energetics of tidal and wind mixing. *Deep-Sea Res.* **45**, 1976–2009.

Nilsson, J. and Walin, G. 2001. Freshwater forcing as a booster of thermohaline circulation. *Tellus* **53A**, 629–641.

Nilsson, J., Broström, G. and Walin, G. 2003. The thermohaline circulation and vertical mixing: does weaker density stratification give stronger overturning? *J. Phys. Oceanogr.* **33**, 2781–2795.

Oberhuber, J. M. 1993. Simulation of the Atlantic circulation with a coupled sea ice-mixed layer isopycnal general circulation model. Part I: model description. *J. Phys. Oceanogr.* **23**, 808–829.

Palmer, T. N. 1999. A nonlinear dynamical perspective on climate prediction. *J. Climate* **12**, 575–591.

Paparella, F. and Young, W. R. 2002. Horizontal convection is non-turbulent. *J. Fluid Mech.* **466**, 205–214.

Pasquero, C. and Tziperman, E. 2004. Effects of a wind-driven gyre on themohaline circulation variability. *J. Phys. Oceanogr.* **34**, 805–816.

Pedlosky, J. 1996. *Ocean Circulation Theory*. Springer-Verlag, Berlin, 450 pp.

Sandström, J. W. 1908. Dynamicsche Versuche mit Meerwasser. *Annalen der Hydrographie under Martimen Meteorologie* **36**, 6–23.

Stern, M. E. 1975. *Ocean Circulation Physics*. Academic, New York, 246 pp.

Stommel, H. 1961. Thermohaline convection with two stable regimes of flow. *Tellus* **13**, 131–149 (S61).

Stommel, H. and Rooth, C. 1968. On the interaction of gravitational and dynamic forcing in simple circulation models. *Deep-Sea Res.* **15**, 165–170.

Thual, O. and McWilliams, J. C. 1992. The catastrophe structure of themohaline convection in a two-dimensional fluid model and a comparison with low-order box models. *Geophys. Astrophys. Fluid Dyn.* **64**, 67–95.

Tritton, D. J. 1988. *Physical Fluid Dynamics*. 2nd edn, Oxford Univ. Press, Oxford, 519 pp.

Tziperman, E., Toggweiler, J. R., Feliks, Y. and Bryan, K. 1994. Instability of the thermohaline circulation with respect to mixed boundary-conditions—is it really a problem for realistic models? *J. Phys. Oceanogr.* **24**, 217–232.

Wang, Y., Singer, J. and Bau, H. U. 1992. Controlling chaos in a thermal convection loop. *J. Fluid Mech.* **237**, 479–498.

Welander, P. 1967. On the oscillatory instability of a differentially heated fluid loop. *J. Fluid Mech.* **29**, 17–30.

Welander, P. 1985. Thermohaline effects in the ocean circulation and related simple models. In: *Large-Scale Transport Processes in Oceans and Atmosphere*, NATO ASI Series C. Vol. 190, 163–200.

Whitehead, J. A. 1995. Thermohaline ocean processes and models. *Ann. Rev. Fluid Mech.* **27**, 89–113.

Wright, D. G., Stocker, T. F. and Mercer, D. 1998. Closures used in zonally averaged models. *J. Phys. Oceanogr.,* **28**, 791–804.

Wunsch, C. 2002. What is the thermohaline circulation? *Science* **298**, 1180–1181.

Wunsch, C. and Ferrari, R. 2004. Vertical mixing, energy, and the general circulation of the oceans. *Ann. Revs. Fl. Mech.* **36**, doi:10.1146/annurev.fluid.36.050802.122121.

Wunsch, C. 2005. Speculations on a schematic Theory of The Younger Dryas. *J. Mor. Res.* **63** (Fofonoff Vol.), in press.